

First-principle study of Au_nSc_m ($n = 1-7$, $m = 1, 2$) clusters

Gui-Xian Ge, Hong-Xia Yan*, Qun Jing, Hai-Bin Cao, and Jian-Jun Zhang

Key Laboratory of Ecophysics and Department of Physics, Normal College, Shihezi University, Xinjiang 832003, China

Received 10 September 2010; Accepted (in revised version) 15 October 2010

Published online 28 February 2011

Abstract. The geometries, stabilities, electronic, and magnetic properties of Au_nSc_m ($n = 1-7$, $m = 1, 2$) clusters have been systematically investigated by density functional theory. It is shown that the most stable structures of Au_nSc ($n = 1-7$) clusters favor planar structure and Sc atom is prone to occupy the center site of Au atoms ring. For Au_nSc_2 clusters, the $3d$ configurations become the lowest energy structure for $n \geq 3$; the growth is based on triangle bipyramid structure of Au_3Sc_2 cluster except Au_4Sc_2 . The second-order energy difference and the fragmentation energy show Au_3Sc , Au_5Sc , Au_3Sc_2 and Au_6Sc_2 clusters possess relatively higher stabilities than their neighbor size. The doping of Sc atom can greatly improve the stability of Au clusters. The doped one Sc atom changes the odd-even alternation trend of gaps in Au_n . The two doped-Sc atoms enhance chemical activity of Au_n in most cases. The total magnetic moments with even valence electrons are quenched on the whole due to electron pairing effects. The averaged coordination number for Sc should be major reason for reduce of local magnetic moments of Sc atom with cluster size increasing in cluster with odd valence electrons. The total magnetic moments in AuSc and Au_2Sc_2 are no quenched due to the smaller coordination number, the charge transfer and weak hybridization between the Sc and Au atoms.

PACS: 31.15.A-, 36.40.Cg

Key words: Au_nSc_m ($n = 1-7$, $m = 1, 2$) clusters, geometry structure, electronic properties

1 Introduction

Recent experiments have shown that the gold clusters have been aroused considerable interests by chemists and physicists due to their unique physical and chemical properties, particularly, their catalytic activities [1, 2]. Interestingly enough, the activity of gold clusters has

*Corresponding author. *Email address:* geguixian@126.com (G. X. Ge)

been found to depend critically on the size of the particle and the nature of the substrate. For example, when supported on the $\text{Mg}(\text{OH})_2$ surface, the best catalytic activity for oxidation of CO is observed for a system size of 13 atoms [3], while the optimal activity of gold clusters supported on TiO_2 surfaces occurs for sizes of 2–3 nm. Since the chemical and physical properties of gold clusters depend greatly on their physical structures, significant efforts have been made to determine the most stable configurations of gold clusters in this size range.

On the other hand, the structure and electronic properties of the doped clusters are usually different from the pure clusters. Many studies have been performed on impurity-doped or mixed gold clusters in order to enhance the stability of gold clusters and improve their chemical activities, or examine the electronic shell structures in mixed gold clusters [4–6]. For example, Bouwen *et al.* [7] and Heinebrodt *et al.* [8] investigated the bimetallic Au_nX_m^+ clusters ($\text{X}=\text{Cu}, \text{Al}, \text{Y}, \text{In}, \text{Cs}; n=1-65, m=1,2$). Especially, extreme size sensitivity of catalytic activity of supported Au clusters is worthy of particular attention [9]. Guo *et al.* investigated small Au_nNi^- [10], Au_nY_2 ($n=1-4$) [11], Au_nFe ($n=1-7$) [12], Au_nPd^- [13] and Au_nPd_2 [14] using the density functional method B3LYP with relativistic effective core potentials (RECP) and LANL2DZ basis set. Garzn *et al.* [15] investigated small Au_nS ($n=1-5$) and Au_nS_2 ($n=1-4$) clusters. Yuan *et al.* investigated geometric, electronic, and bonding properties of Au_NM ($N=1-7, \text{M}=\text{Ni}, \text{Pd}, \text{Pt}$) clusters [16], and found that the dopant atoms markedly change the geometric and electronic properties of gold clusters. Zhang *et al.* investigated the geometries, electronic, and magnetic properties of the 3d transition-metal-doped gold cluster: M@Au_6 clusters ($\text{M}=\text{Sc}, \text{Ti}, \text{V}, \text{Cr}, \text{Mn}, \text{Fe}, \text{Co}, \text{Ni}$) [17]. Torres *et al.* [18] investigated the structural, electronic, and magnetic properties of Au_nM^+ clusters ($\text{M}=\text{Sc}, \text{Ti}, \text{V}, \text{Cr}, \text{Mn}, \text{Fe}, \text{Au}; n \leq 9$) using first-principles density functional calculations in which the magnetic moment showed pronounced odd-even effects as a function of the cluster size and resulted in values very sensitive to the geometrical environment. Neukermans and co-workers [19, 20] have investigated the stability of cationic gold clusters doped with a 3d TM atom, Au_nTM^+ , with TM from Sc to Zn, and extended their investigations to multiply TM atoms doped gold clusters Au_NX_M clusters ($\text{X}=\text{Sc}, \text{Ti}, \text{Cr}, \text{Fe}; N=1-40, M=0-3$) by means of photofragmentation experiments [21].

Although there has been a substantial amount of research for doped gold clusters. No systematic studies on Sc-doped gold clusters have been reported to our knowledge. In this paper, we will provide an *ab initio* structural and electronic investigation for Au_nSc_m ($n=1-7, m=1,2$) clusters by using density functional theory. This information will be useful to understand the enhanced catalytic activity and selectivity gained by using Sc-doped gold catalyst. In order to examine the effect of Sc atom to gold clusters, geometry optimizations of pure gold clusters were also calculated using identical method. The rest of the paper is organized as follows: In Section 2, the calculation details are described. Section 3 presents the results and discussion. Finally, the summary and conclusions are given in Section 4.

2 Computational method

Full geometry optimizations were performed using density functional theory (DFT) in a DMOL³ package [22]. In the electronic structure calculations, all electron treatment and double numerical basis including d-polarization function (DNP) [22] were chosen. The relativistic effects are very important for Au-type high Z system in defining geometric properties [23–25]. Therefore our calculations are carried out using the relativistic scheme. The exchange-correlation interaction was treated within the generalized gradient approximation (GGA) using BLYP functional. Self-consistent field calculations were done with a convergence criterion of 10^{-5} hartree on the total energy. The density mixing criterion for charge and spin were 0.2 and 0.5, respectively. The Direct Inversion in an Iterative Subspace (DIIS) approach was used to speed up SCF convergence. A 0.001 hartree of smearing was applied to the orbital occupation. In the geometry optimization, the converged thresholds were set to 0.004 hartree/Å for the forces, 0.005 Å for the displacement and 10^{-5} hartree for the energy change.

Harmonic vibrational frequencies were calculated for the promising stationary points from a direct structural optimization; if an imaginary vibrational mode was found, a relaxation along coordinates of imaginary vibrational mode was carried out until the true local minimum was actually obtained. Therefore, all isomers for each cluster are guaranteed as the local minima. The on-site charges and magnetic moment were evaluated via Mulliken population analysis [26]. To test the accuracy of the theoretical method, the dimers for Au₂, Sc₂ and AuSc have been calculated by using different functionals. For Au₂, the bond length $r = 2.52$ Å, $E_b = 2.29$ eV, $\omega = 169.06$ cm⁻¹; the calculated results using BLYP functional are in good agreement with the experimental data ($r = 2.47$ Å, $E_b = 2.30$ eV, $\omega = 191$ cm⁻¹) [27, 28]. For Sc₂, the computed binding energy of 1.54 eV is well reproduced in comparison with the measured values of 1.65 ± 0.22 eV [29, 30]. For AuSc, the bond length $r = 2.55$ Å, $\omega = 234.97$ cm⁻¹, the calculated results are in good agreement with the previous theory values [31]. It indicates that the employed BLYP scheme is reliable for Au₂, Sc₂ and AuSc dimers. Thus, one may expect that it can also yield accurate prediction for Au_{*n*} and Au_{*n*}Sc_{*m*} clusters in this paper.

3 Results and discussion

3.1 Growth pattern

The stable structures of Au_{*n*} and Au_{*n*}Sc_{*m*} clusters are shown in Figs. 1–3. Although we obtained a lot of stable structures for Au_{*n*} and Au_{*n*}Sc_{*m*} clusters at each size, we do not show all of them in the figures for the sake of simplicity. The structures of Au_{*n*} and Au_{*n*}Sc_{*m*} clusters are denoted by arabic number and letter, where the arabic number denotes the Au atom number and the letter ranks the isomers in decreasing order of binding-energy.

3.1.1 Au_{*n*} clusters

The lowest energy geometry of Au₃ is an obtuse triangle with the angle of 139.61°, which is identical to Idrobos' result [32]. The metastable isomer is an equilateral triangle with Au-Au

bond lengths of 2.67 Å and its energy is 0.14 eV higher than the lowest energy structure. A rhombus is the lowest energy structure of Au₄. The lowest energy structure of Au₅ is a planar structure obtained by one Au atom capped on the lowest energy structure of Au₄. In agreement with the earlier results, the lowest energy geometry of Au₆ is an equilateral triangle embedded in a bigger one. The other isomers are also presented in Fig. 1. For Au₇, the lowest energy structure is different from those of empirical methods by Shafai *et al.* [33] who has concluded that the lowest energy structure of Au₇ is a pentagonal bipyramid. The lowest energy configuration we obtained is planar capped triangle whose binding energy is 1.20 eV lower than the pentagonal bipyramid. The most stable structure of Au₇ is 0.67 eV lower than a hexagon with one gold atom occupying the center of the ring (7B in Fig. 1). The lowest energy structures of Au_n ($n=2-7$) are all planer structure and the results are almost consistent with the previous results [34].

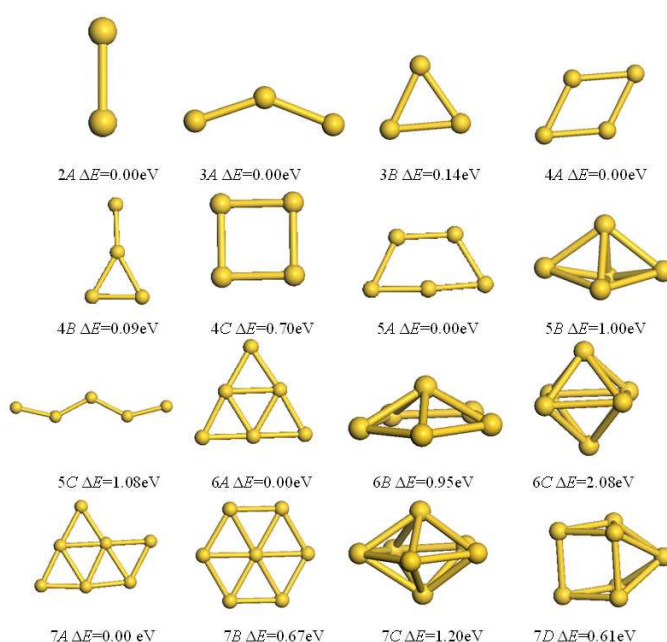


Figure 1: The lowest energy and some metastable geometries of Au_n clusters. ΔE is the excess energy of an isomer as compared to the energy of the most stable one.

3.1.2 Au_nSc clusters

The lowest-energy and some metastable structures of Au_nSc clusters are shown in Fig. 2. The triangle structure with apex angles of 176.67° (2a in Fig. 2) with quintet spin state is found to be the lowest energy structure of Au₂Sc cluster, which is energetically lower than the same structure with other spin states. For Au₃Sc cluster, "Y-shaped" structure obtained with the Sc atom at the center is the lowest structure with D_{3h} symmetry. The lowest energy structure of Au₃Sc cluster is different from Au₃Ni⁻ [10], Au₃Fe [12] and Au₃Pd⁻ [13], and is

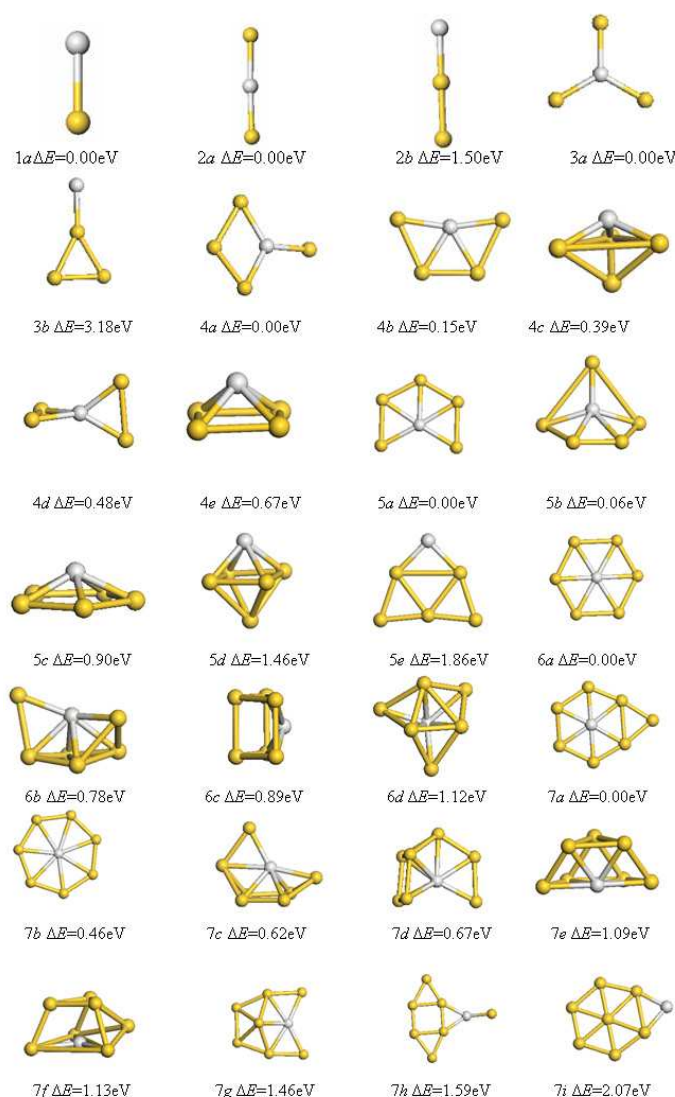


Figure 2: The lowest energy and some metastable geometries of Au_nSc clusters. The yellow circles are the Au atoms while the white circles are the Sc atoms. ΔE is the excess energy of an isomer as compared to the energy of the most stable one.

identical to Au_3Y [35]. Another "Y-shaped" structure with the Sc atom occupying apex position is obtained, and its energy is higher than the lowest energy structure by 1.50 eV. The most stable structure for Au_4Sc cluster originates from capping an Au atom on the side of the Au_3Sc isomer (3a in Fig. 2), which is different from Au_4Ni^- [10], Au_4Fe [12] and Au_4Pd^- [13], and is identical to Au_4Y [35]. A planar trapezoidal shaped with Sc centered in the middle of bottom lateral is low-lying isomer which is higher than the lowest energy structure by 0.15 eV. The 4c isomer is a 3D structure with Cs symmetry and its energy is higher than the lowest

energy structure by 1.50 eV. The total energies of other two isomers (4d, and 4e in Fig. 2) are higher than the lowest energy structure by 0.48 and 0.67 eV, respectively. In the case of Au₅Sc cluster, the lowest energy structure corresponds to a planar configuration with the impurity atom occupying center position, which is the second isomer in the Au₅Fe cluster optimizations [12]. A planar configuration with the impurity atom occupying apex position is 1.86 eV less stable than the lowest energy configuration.

In our calculations for the Au₅Sc, the 3-D structures (5b, 5c, 5d in Fig. 2) are the low-lying isomers with energy differences of 0.06, 0.90 and 1.46 eV, respectively. The lowest energy structure of Au₆Sc is planar hexagon with the impurity atom located at the center site, which can be derived from the pentagonal isomer of Au₅Sc. The lowest energy structure of Au₆Sc is similar to Au₆Fe [12], Au₆Pd [16], Au₆Pt [16] and Au₆Ni [16]. The structure formed by two Au atoms capping on the 5d (6b in Fig. 1) is 0.78 eV higher in energy compared to the lowest energy structure. Other two 3D isomers are less stable than the lowest energy structure with 0.89 and 1.12 eV, respectively. For Au₇Sc, the planar structure derived from 6a by adding a gold atom to one side is the lowest energy structure, which is similar to Au₇Fe [12], Au₇Pd [16], Au₇Pt [16] and is different from Au₇Ni [16]. The planar structure with Sc atom occupying side position is higher than the lowest energy structure by 2.07 eV. Another planar structure with Sc atom located at the center site of seven atoms ring is 0.46 eV less stable than the lowest energy configuration. Other 3D isomers are shown in Fig. 2. As is discussed above, the most stable structures of Au_nSc clusters favor planar structure and Sc atom is prone to occupy the center site of Au atoms ring. The coordination number of Sc atom increases with the size of cluster and reach to a stable coordination number 6. The doped Sc atom does not disturb the frame of Au_n clusters.

3.1.3 Au_nSc₂ clusters

Fig. 3 shows the optimized results of the Au_nSc₂ clusters. The most stable structure of AuSc₂ is a triangular(C_{2v}) configuration. The linear structures with Sc-Sc bond and central Au atom are optimized. Both structures are confirmed as local minima. Among them, the geometry breaking the Sc₂ bond is the least stable. For Au₂Sc₂ cluster, the rhombus structure with D_{2h} symmetry is the most stable isomer as it is also occurred in the Au₄ cluster optimizations. Another rhombus structure with C_{2v} symmetry is higher than the lowest energy structure by 0.06 eV. Isomer 2II (in Fig. 3) is a three-dimensional structure, which is a butterfly like structure with Sc-Sc cross-bonding, and its energy is 0.05 eV higher than the lowest energy structure. Other two planar isomers are less stable with 0.50 and 1.06 eV, respectively. In the case of Au₃Sc₂ cluster, a triangle bipyramid structure with Sc atom occupying apex position is the lowest energy structure which is 0.94 eV lower than triangle bipyramid structure with two Sc atoms located at a planar triangle site. Two butterfly like structures are found, one derived from 2I by adding a gold atom to one end of Sc atom, other derived from 2I by adding a gold atom to one side. The former is 0.09 eV lower than the latter. However, two planar isomers are 0.97 and 1.08 eV higher in energy than the most stable structure. The lowest energy structure of Au₄Sc₂ cluster can be obtained by adding a gold atom to one end of another Sc atom in 3II (in Fig. 3). The triangle bipyramid structure derived from 3I by adding a gold

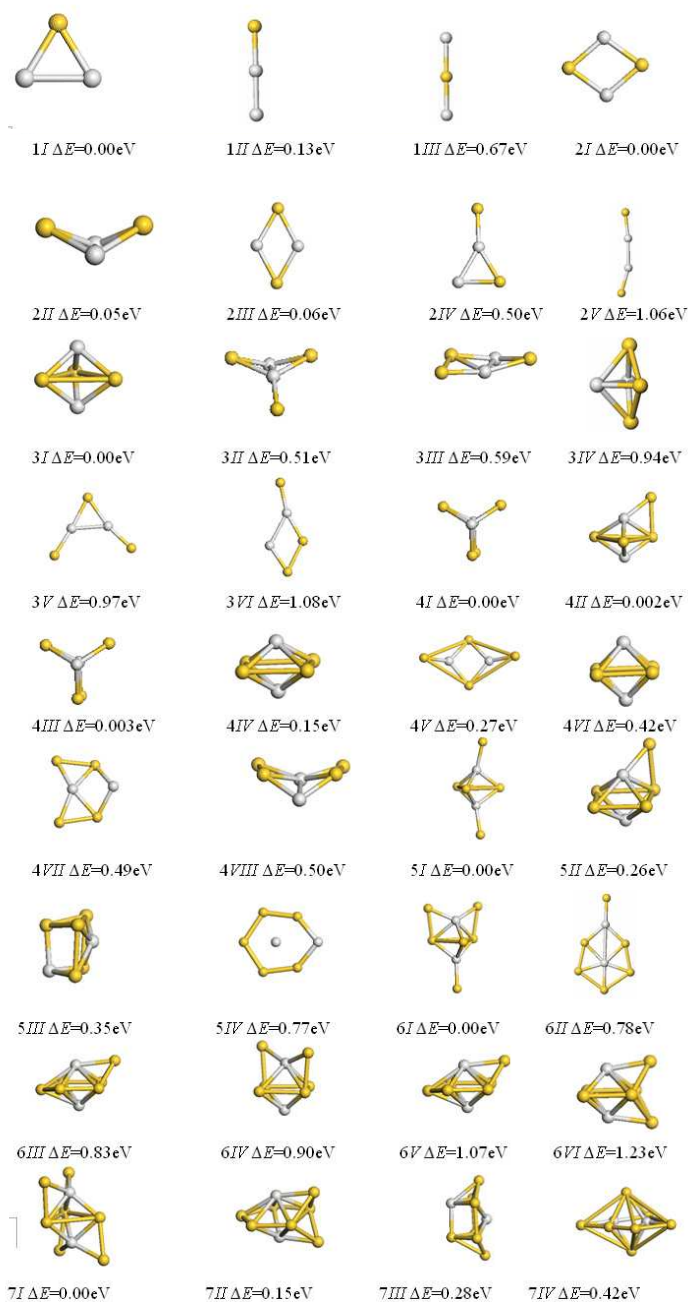


Figure 3: The lowest energy and some metastable geometries of Au_nSc_m clusters. The yellow circles are the Au atoms while the white circles are the Sc atoms. ΔE is the excess energy of an isomer as compared to the energy of the most stable one.

atom to one side is only higher than the lowest energy structure by 0.002 eV. Isomer *3III* has a similar geometrical structure as isomer *3I*, but its energy is higher 0.003 eV compared with *3I*.

Two square bipyramid isomers are found and their energies are 0.15 and 0.42 eV higher than the most stable structure, respectively. With regard to the Au_5Sc_2 cluster, the lowest energy structure is derived from *3I* by adding two gold atoms to one end of two Sc atoms. The square bipyramid by adding a gold atom to one side in *4IV* is less than *5I* isomer by 0.26 eV. Other isomers (*5III* and *5VI* in Fig. 3) are higher than that of the lowest energy structure by 0.35 and 0.77 eV, respectively. The structure *6I*, which is obtained by adding two gold atoms to one side of one Sc atom and one gold atom to one end of other Sc atom, is the most stable structure of Au_6Sc_2 . The planar isomer *6II* is 0.78 eV higher than the lowest energy structure. Other 3D structure isomers are higher than that of the lowest energy structure by 0.83, 0.90, 1.07 and 1.23 eV, respectively. The most stable structure of Au_7Sc_2 is *7I*, which is derived from *3I* by adding two gold atoms to one side of two Sc atoms, respectively. The lowest energy structure is 0.15 eV lower in energy than the *7II* isomer obtained by capping a gold atom on *6V*. *7III* and *7IV* are higher than that of the lowest energy structure by 0.28 and 0.42 eV, respectively. The most stable structures of Au_nSc_2 clusters ($n \leq 2$) are planar structure; the 3D configurations become the lowest energy structure for the Au_nSc_2 clusters ($n \geq 3$), whose growth is based on triangle bipyramid structure of Au_3Sc_2 cluster except for Au_4Sc_2 .

3.2 Relatives and electronic properties

We now discuss the relative stability of Au_nSc_m ($n = 1-7$, $m = 1, 2$) clusters. The relative stability of differently sized clusters can be predicted by calculating the average binding energy of total energies $E(n)$. The averaged binding energies for Au_n and Au_nSc_m ($m = 1, 2$) clusters can be defined as the following formula

$$E_b(n) = \frac{(-E_T[\text{Au}_n] + nE_T[\text{Au}])}{n}, \quad (1)$$

$$E'_b(n) = \frac{(-E_T[\text{Au}_n\text{Sc}] + nE_T[\text{Au}] + mE_T[\text{Sc}])}{(n+m)}, \quad (2)$$

where $E_T[\text{Au}_n]$, $E_T[\text{Au}_n\text{Sc}_m]$, $E_T[\text{Au}]$ and $E_T[\text{Sc}]$ represent the total energies of the Au_n , Au_nSc_m , Au and Sc, respectively. The average binding energies for Au_n and Au_nSc_m are shown in Fig. 4. For Au_nSc clusters, the binding energy curve gradually increases at $n \leq 3$, but decreases at $n = 4$, and forms peak at $n = 3$, implying that Au_3Sc cluster is more stable. For $n > 4$, the binding energies of Au_nSc clusters stay nearly constant. The average binding energies of Au_nSc_2 clusters increase gradually in the range $n = 2-6$. The curve of $E_b(n)$ exhibits a prominent peak at $n = 6$, indicating that Au_6Sc_2 possesses unusually high stability. Moreover, the average binding energies of Au_nSc_m ($m = 1, 2$) are far higher than those of Au_n clusters at smaller sizes, indicating the doping of Sc atoms can greatly improve the stability of Au clusters with smaller sizes.

To further illustrate the stability of the cluster and the size-dependent behavior, we investigate the second difference in energy as a function of size. The $\Delta_2 E$ is a quantity frequently used as a measure of the relative stability of the cluster and is often compared directly with

the relative abundances determined in mass spectroscopy experiments. It is defined as

$$\Delta_2 E(n) = E(n+1) + E(n-1) - 2E(n) \quad (3)$$

where $E(n)$ is the total energy of an n -atom cluster. For Au_n clusters, as shown in Fig. 5, particularly prominent maxima for are found at $n=2,4,6$, indicating these clusters are more stable than their neighbors. In the case of Au_nSc , two prominent maxima are found at $n=3$ and 5. Consequently, it can be deduced that the Au_3Sc and Au_5Sc clusters possess relatively higher stability. The peaks for Au_nSc_2 are found at $n=3,6$, indicating that these clusters are more stable than their neighbors.

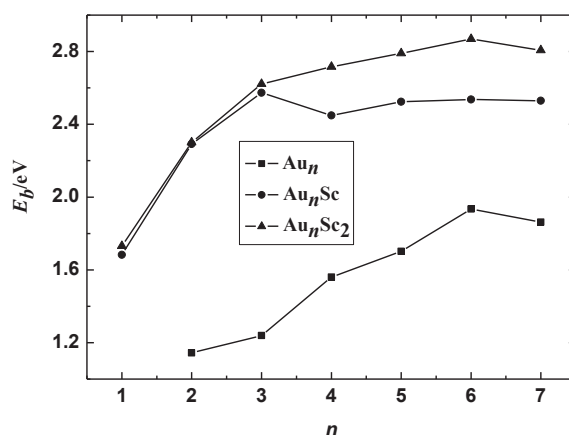


Figure 4: Binding energy versus cluster size for Au_n and Au_nSc_m clusters.

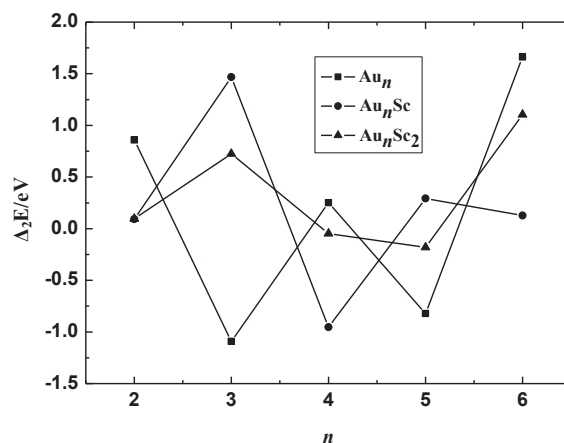


Figure 5: Second finite difference of the total energies for Au_n and Au_nSc_m clusters.

The fragmentation energy (E_F) is another useful quantity for determining the stability of clusters. The fragmentation energy of the total energies for Au_n and Au_nSc_m ($m=1,2$) clusters

are presented in Fig. 6. The fragmentation energy can be defined by the following formula

$$E_F = E_T[\text{Au}] + E_T[\text{Au}_{n-1}] - E_T[\text{Au}_n], \quad (4)$$

$$E'_F = E_T[\text{Au}] + E_T[\text{Au}_{n-1}\text{Sc}_m] - E_T[\text{Au}_n\text{Sc}_m], \quad (5)$$

where $E_T[\text{Au}]$, $E_T[\text{Au}_{n-1}]$, $E_T[\text{Au}_{n-1}\text{Sc}_m]$, $E_T[\text{Au}_n\text{Sc}_m]$ and $E_T[\text{Au}_n]$ represent the total energies of Au, Au_{n-1} , $\text{Au}_{n-1}\text{Sc}_m$, Au_nSc_m and Au_n , respectively. As shown in Fig. 6, the local peaks of $E_F(n)$ for Au_n appear at the sizes of 2, 4 and 6, suggesting these clusters are more stable than their neighboring size. For Au_nSc , the local maxima of $E_F(n)$ appear at the sizes of 3 and 5, showing these clusters are more stable, which is consistent with the result of Δ_2E . In the case of Au_nSc_2 , the values of Au_3Sc_2 and Au_6Sc_2 are larger than their neighboring size, so these clusters are more stability than neighboring clusters, which is also consistent with the result of Δ_2E shown in Fig. 5.

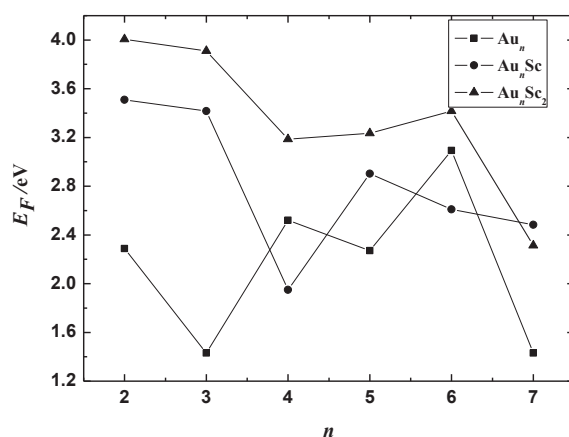


Figure 6: The fragmentation energy of the total energies for Au_n and Au_nSc_m clusters.

The HOMO-LUMO gap is a characteristic quantity of metal clusters' electronic structure and is a commonly used measure of the ability for clusters to undergo activated chemical reactions with small molecules. For the lowest energy structures of Au_nSc_m ($n=1-7$; $m=1,2$) clusters, the HOMO-LUMO gaps are shown in Fig. 7. For Au_n , the gaps appear odd-even alternation, the values of even number cluster are larger than that of neighboring odd number cluster. Namely, the gaps for the Au_n clusters with even electronic numbers are larger than those with odd electronic numbers. The valence electronic configuration of Au is $4f^{14}5d^{10}6s^1$. There are full sharing electrons for the clusters with even number which corresponds to the close-shell structure, so their chemical activities are comparatively weaker than those of the clusters with odd number electrons. So electron-pairing effect governs such odd-even alternation, and this explanation has been based on the presupposition of valance electron delocalization. The HOMO-LUMO gaps of Au_nSc appear also odd-even alternation, but the values of even number cluster are smaller than that of neighboring odd number clusters. The valence electronic configuration of Sc is $3d^1s^2$, when Sc is doped on the Au_n clusters, cluster geometry

does dominate positive role in enhancing their stability. For Au_nSc_2 , the trends in energy gap are similar to those of Au_n clusters, but the values are smaller than corresponding Au_n clusters except for Au_7Sc_2 , which means two doped Sc atoms enhance chemical activity of Au_n in most cases.

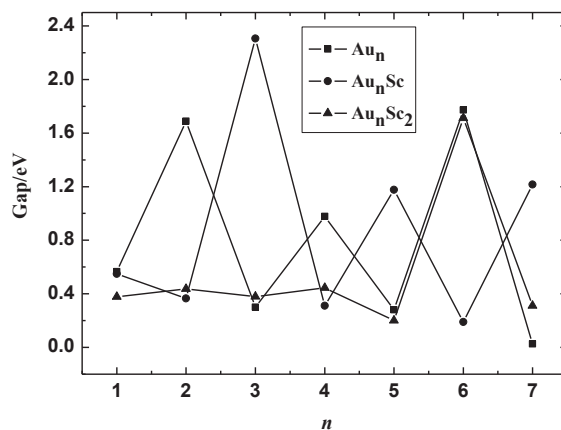


Figure 7: The HOMO-LUMO Gaps of the total energies for Au_n and Au_nSc_m clusters.

3.3 Magnetic properties

The total magnetic moments of the lowest energy structures of Au_nSc_m ($n = 1-7$; $m = 1, 2$) clusters have been calculated and the results are presented in Table 1. For Au_nSc , the total magnetic moments appear odd-even alternation, the electronic configuration of Sc is $3d^{14}s^2$, so the total magnetic moments are quenched with odd Au atoms clusters due to electron pairing effects except that the total magnetic moment of $AuSc$ is $2\mu_B$. The total magnetic moments are $1\mu_B$ with even Au atoms clusters. The local spin moments of Sc atom are found to align ferromagnetically to the Au atoms with even Au atoms clusters except that the local magnetic moments of the Sc site appear antiferromagnetic alignment in Au_2Sc . For $AuSc$ and Au_2Sc , the local magnetic moments are mainly located on the Sc sites, while for Au_4Sc and Au_6Sc , the local magnetic moments are mainly located on the Au sites. In the case of Au_nSc_2 , the total magnetic moments also appear odd-even alternation except Au_2Sc_2 which the total magnetic moment is $2\mu_B$. The total magnetic moments of Au_nSc_2 with odd Au atom are $1\mu_B$, and the total magnetic moments are quenched with even Au atom. The local spin moments of Sc atoms are also found to align ferromagnetically to the Au atoms for the cluster with even Au atoms. The local magnetic moments are mainly located on the Sc sites except Au_7Sc . As can be seen from Table 1, the local magnetic moments on the Sc sites for Au_nSc_m are gradually reducing with cluster size increasing on the whole except that local magnetic moments on the Sc sites are quenched. To further understand this effect, we analyze the averaged coordination number for Sc. Generally speaking, the lower coordination number of atomic clusters, the localized d state is the more narrow and thus the d electronic

Table 1: Symmetries, bond length between Sc and Au (\AA), average coordination numbers (CN), atomic charges (e) at the Sc atom, magnetic moment (μ_B) of the Sc atom, and the total magnetic moment (μ_B) of Au_nSc_m clusters for the lowest-energy structures.

Cluster	Symm.	$r_{\text{Sc-Au}}$	N	Charge on Sc	Magnetic moment on Sc	Total magnetic moment
AuSc	C_{1v}	2.545	1	0.439	1.935	2.000
Au ₂ Sc	C_{2v}	2.585	2	0.872	1.042	1.000
Au ₃ Sc	D_{3h}	2.516	3	1.057	0.000	0.000
Au ₄ Sc	C_1	2.618	4	1.035	0.233	1.000
Au ₅ Sc	C_1	2.689	5	1.063	0.000	0.000
Au ₆ Sc	C_1	2.706	6	1.087	0.099	1.000
Au ₇ Sc	C_1	2.729	6	1.089	0.000	0.000
AuSc ₂	C_{2v}	2.676	1.5	0.218	0.882	1.000
Au ₂ Sc ₂	D_{2h}	2.630	2	0.424	1.768	2.000
Au ₃ Sc ₂	C_{2v}	2.659	3	0.551	0.867	1.000
Au ₄ Sc ₂	C_1	2.702	3.5	0.758	0.000	0.000
Au ₅ Sc ₂	C_1	2.648	4	0.887	0.830	1.000
Au ₆ Sc ₂	C_5	2.665	4.5	0.961	0.000	0.000
Au ₇ Sc ₂	C_1	2.700	5	0.974	0.240	1.000

Table 2: The charge (e) and magnetic moment (μ_B) of 3d, 4s, and 4p states for Sc atom in Au_nSc_m ($n=1-7, m=1,2$) clusters.

Cluster	3d		4s		4p	
	Charge	Magnetic moment	Charge	Magnetic moment	Charge	Magnetic moment
AuSc	1.433	-1.138	1.031	-0.738	0.104	-0.058
Au ₂ Sc	1.517	1.012	0.421	0.020	0.008	0.199
Au ₃ Sc	1.263	0.000	0.391	0.000	0.317	0.000
Au ₄ Sc	1.327	0.198	0.348	0.024	0.312	0.011
Au ₅ Sc	1.360	0.000	0.287	0.000	0.310	0.000
Au ₆ Sc	1.400	0.095	0.228	0.002	0.304	0.002
Au ₇ Sc	1.371	0.000	0.245	0.000	0.314	0.000
AuSc ₂	1.444	0.125	1.192	0.432	0.149	0.020
AuSc ₂	1.439	-0.119	1.205	0.400	0.146	0.023
Au ₂ Sc ₂	1.336	0.689	1.074	0.174	0.175	0.019
Au ₂ Sc ₂	1.335	0.693	1.077	0.172	0.174	0.019
Au ₃ Sc ₂	1.313	0.403	0.917	0.020	0.232	0.005
Au ₃ Sc ₂	1.309	0.412	0.927	0.020	0.231	0.006
Au ₄ Sc ₂	1.479	0.000	0.640	0.000	0.223	0.000
Au ₄ Sc ₂	1.544	0.000	0.357	0.000	0.256	0.000
Au ₅ Sc ₂	1.425	0.376	0.370	0.021	0.331	0.017
Au ₅ Sc ₂	1.421	0.371	0.378	0.027	0.331	0.016
Au ₆ Sc ₂	1.411	0.000	0.271	0.000	0.354	0.000
Au ₆ Sc ₂	1.335	0.000	0.400	0.000	0.354	0.000
Au ₇ Sc ₂	1.391	0.107	0.299	0.002	0.299	0.002
Au ₇ Sc ₂	1.392	0.106	0.299	0.002	0.357	0.011

state is more prone to have more spin-spin splitting to form a larger magnetic moment. It clearly shows that the averaged coordination numbers of Au_nSc_m increase with cluster size increasing, which is one reason that the local magnetic moments on the Sc sites for Au_nSc_m

are gradually reducing with cluster size increasing on the whole. The quenched magnetic moment of Au_nSc_m can be explained by electron pairing effects except AuSc and Au_2Sc_2 . In order to explain this effect, we performed Mulliken population analysis for the lowest energy structures and the atomic charges of Sc atom in the Au_nSc_m clusters are listed in Table 1. For all clusters the charges transfer from Sc atoms to Au atoms and the amount of charge transfer increases with increasing cluster size on the whole. The charges on Sc atoms for AuSc and Au_2Sc_2 are smaller than that of Au_nSc with odd Au atoms and Au_nSc_2 with even Au atoms, respectively. Smaller coordination number and the charge transfer may be the reason that the total magnetic moments of AuSc and Au_2Sc_2 are not quenched. To further understand this effect, we have analyzed the on-site atomic charges and local magnetic moment. The charge and spin of $3d$, $4s$ and $4p$ states for Sc atom in the Au_nSc_m clusters are summarized in Table 2. It clearly shows that the magnetic moment of the Sc atom is mainly due to $3d$ state of Sc. For free Sc atom, the configuration of valence electrons is $3d^24s^1$. In the cases of the Au_nSc_m clusters, the $4s$ state always loses electrons, the $3d$ and $4p$ states always gain some amount of electrons. There is internal electron transfer between $4s$ state and $3d$, $4p$ states in the Sc atom, which indicates there is internal hybridization in Sc atom. Combined with the results mentioned above (Table 2) that there is charge transfer between Sc atom and Au atoms. The charge transfers between the Sc and Au atoms in AuSc and Au_2Sc_2 are smaller than that of Au_nSc with odd Au atoms and Au_nSc_2 with even Au atoms, which suggests the weaker hybridization between the Sc and Au atoms causes no quenched magnetic moment, respectively.

4 Conclusion

By using first-principles DFT-GGA calculations, the geometries, stabilities, and magnetic properties of the Au_nSc_m clusters have been systematically studied. The results are summarized as follows:

1. The most stable structures of Au_nSc clusters favor planar structure and Sc atom is prone to occupy the center site of Au atoms ring. The coordination number of Sc atom increases with the size of cluster and reach to a stable coordination number 6. The doped Sc atom does not disturb the frame of Au_n clusters. For Au_nSc_2 clusters, the most stable structures for $n \leq 2$ are planar structure; the $3d$ configurations become the lowest energy structure for $n \geq 3$; the growth is based on triangle bipyramid structure of Au_3Sc_2 cluster except for Au_4Sc_2 .
2. From the analysis of the second-order energy difference, the fragmentation energies, Au_3Sc , Au_5Sc , Au_3Sc_2 and Au_6Sc_2 clusters possess relatively higher stabilities than their neighbor size.
3. The doping of Sc atom can greatly improve the stability of Au clusters with smaller sizes. The doped one Sc atom changes the odd-even alternation trend of gaps in Au_n . The two doped-Sc atoms enhance chemical activity of Au_n in most cases.
4. The total magnetic moments with even valence electrons are quenched on the whole

due to electron pairing effects. The averaged coordination number for Sc should be major reason for the reduce of local magnetic moments in Sc atom with cluster size increasing in cluster with odd valance electrons. The total magnetic moments in AuSc and Au₂Sc₂ are no quenched due to the smaller coordination number, the charge transfer and weak hybridization between the Sc and Au atoms.

Acknowledgments. The authors acknowledge the computational support from the Institute of Theoretical Physics of Henan University.

References

- [1] G. Bravo-Pérez, I. L. Garzón, and O. Novaro, *J. Mol. Struct. (Theochem.)* 493 (1999) 225.
- [2] G. Bravo-Pérez, I. L. Garzón, and O. Novaro, *Chem. Phys. Lett.* 313 (1999) 655.
- [3] D. A. H. Cunningham, W. Vogel, H. Kageyama, *et al.*, *J. Catal.* 177 (1998) 1.
- [4] K. Koszinowski, D. Schröder, and H. Schwarz, *Chem. Phys. Chem.* 4 (2003) 1233.
- [5] H. Häkkinen, S. Abbet, A. Sanchez, *et al.*, *Angew. Chem. Int. Ed.* 42 (2003) 1297.
- [6] P. Pyykkö and N. Runeberg, *Angew. Chem. Int. Ed.* 41 (2002) 2174.
- [7] W. Bouwen, F. Vanhoutte, F. Despa, *et al.*, *Chem. Phys. Lett.* 314 (1999) 227.
- [8] M. Heinebrodt, N. Malinowski, F. Tast, *et al.*, *J. Chem. Phys.* 110 (1999) 9915.
- [9] A. Sanchez, S. Abbet, U. Heiz, *et al.*, *J. Phys. Chem. A* 103 (1999) 9573.
- [10] J. J. Guo, J. X. Yang, and D. Die, *J. Mol. Struct. (Theochem.)* 896 (2009) 1.
- [11] J. J. Guo, J. X. Yang, and D. Die, *Physica B* 403 (2008) 4033.
- [12] D. Die, X. Y. Kuang, J. J. Guo, and B. X. Zheng, *J. Mol. Struct. (Theochem.)* 902 (2009) 54.
- [13] J. J. Guo, J. Shi, J. X. Yang, and D. Die, *Physica B* 393 (2007) 363.
- [14] J. J. Guo, J. Shi, J. X. Yang, and D. Die, *Physica B* 367 (2005) 158.
- [15] G. B. Péreza, and I. L. Garzón, *J. Mol. Struct. (Theochem.)* 619 (2002) 79.
- [16] D. W. Yuan, Y. Wang, and Z. Zeng, *J. Chem. Phys.* 122 (2005) 114310.
- [17] M. Zhang, L. M. He, L. X. Zhao, *et al.*, *J. Phys. Chem. C* 113 (2009) 6491.
- [18] M. B. Torres, *Phys. Rev. B* 71 (2005) 155412.
- [19] S. Neukermans, E. Janssens, H. Tanaka, *et al.*, *Phys. Rev. Lett.* 90 (2003) 033401.
- [20] H. Tanaka, S. Neukermans, E. Janssens, *et al.*, *J. Chem. Phys.* 119 (2003) 7115.
- [21] E. Janssens, H. Tanaka, S. Neukermans, *et al.*, *Phys. Rev. B* 69 (2004) 085402.
- [22] B. Delley, *J. Chem. Phys.* 92 (1990) 508.
- [23] H. Häkkinen, M. Moseler, and U. Landman, *Phys. Rev. Lett.* 89 (2002) 033401.
- [24] J. Li, X. Li, H. J. Zhai, and L. S. Wang, *Science* 299 (2003) 864.
- [25] X. Gu, M. Ji, S. H. Wei, and X. G. Gong, *Phys. Rev. B* 70 (2004) 205401.
- [26] R. S. Mulliken, *J. Chem. Phys.* 23 (1955) 1841.
- [27] R. C. Weast, *CRC Handbook of Chemistry and Physics*, 55th ed. (CRC Press, Cleveland, 1974).
- [28] M. G. Hill, *American Institute of Physics Handbook* (CRC Press, New York, 1972).
- [29] M. Moskovits, D. P. DiLella, and W. J. Limm, *J. Chem. Phys.* 80 (1984) 626.
- [30] K. A. Gingerich, *Faraday Symp. Chem. Soc.* 14 (1980) 109.
- [31] Z. J. Wu, *Chem. Phys. Lett.* 406 (2005) 24.
- [32] J. C. Idrobo, W. Walkosz, J. F. Yip, *et al.*, *Phys. Rev. B* 76 (2007) 205422.
- [33] G. S. Shafai, S. Shetty, S. Krishnamurty, *et al.*, *J. Chem. Phys.* 126 (2007) 014704.
- [34] J. L. Wang, G. H. Wang, and J. J. Zhao, *Phys. Rev. B* 66 (2002) 035418.
- [35] H. P. Mao, H. Y. Wang, Z. H. Zhu, and Y. J. Tang, *Acta. Phys. Sin.* 55 (2006) 4542 (in Chinese).